CHAPTER THREE

Modeling Bacteria–Phage Interactions and Its Implications for Phage Therapy

Saptarshi Sinha, Rajdeep K. Grewal, Soumen Roy[1]
Bose Institute, Kolkata, India
[1]Corresponding author: e-mail address: soumen@jcbose.ac.in

Contents

Advances in Applied Microbiology, Volume 103
ISSN 0065-2164
https://doi.org/10.1016/bs.aambs.2018.01.005

Abstract

Bacteriophages are more abundant than any other organism on our planet. The interaction of bacteriophages and bacteria and their coevolution is well known. In this chapter, we describe various aspects of modeling such systems and their dynamics. We explore their interaction in: (i) liquid media, which leads to well-mixed populations and (ii) solid media, where their interaction is spatially restricted. Such modeling, when used in conjunction with experiments would not only shed deep insight into the underlying dynamics but also provide useful clues toward potential therapeutic applications.

1. THE BACTERIA–PHAGE INTERACTION

Bacteriophages, often simply referred to as phages, are perhaps the most abundant and ubiquitous, infectious acellular entities on this planet. Phages are viruses, which need specific bacterial cells to replicate and proliferate. Structurally, like other viruses, bacteriophages are composed of nucleic acids as their core genetic material with an envelope, which is constituted of different types of proteins and glycoproteins. The nucleic acid within a phage particle can be either DNA or RNA. Some unusual features, observed in the genome of a phage like modified bases, help these phage particles in protecting themselves from the defense mechanism of the host. The replication cycle of a DNA virus is much simpler than an RNA virus. Outside the host cell, phage particles appear to behave like nonliving entities, which are unable to reproduce. The typical size of a bacteriophage may vary between 20 and 200 nm in length with a great variety in shapes and in the capsid symmetry—ranging from icosahedral to helical. Phage distributions depend on the distribution of their hosts. As phages need hosts for their replication, their numbers depend on the host cell density in the environment. The maximum number of phages is found in the marine ecosystem. Interestingly, the estimated aggregate number of phage particles on the earth is higher than every other organism on the planet (Mc Grath & van Sinderen, 2007).

1.1 Discovery of Bacteriophages: A Brief History

It was not till the second decade of the 20th century that existence of phages was clearly uncovered. The first unambiguous mention of bacteriophages in line with the conception that we have of them today can be traced to the French-Canadian microbiologist Felix d'Herelle (d'Herelle, 1917) who worked at the Pasteur Institute in Paris. d'Herelle also demonstrated the therapeutic potential of bacteriophages. Indeed he was the one who coined the name bacteriophage (literally bacteria eater), where phage originates from Greek and means "to eat" or "devour." This is especially remarkable given that the autodidact d'Herelle had to face prolonged and significant opposition from some of the powerful scientific minds of his time as well documented in literature (Duckworth, 1976; Summers, 2012).

Before this, however, Ernest Hanbury Hankin reported about unknown things in the river waters of Ganga (Ganges) and Jumna (Yamuna) in India, which could pass through fine porcelain filters and, possessed notable antimicrobial or antibacterial properties especially against cholera (Hankin, 1896). The results seem to be widely known at that time and even find a mention in Mark Twain's famous travelogues (Twain, 1897). However, recent works (Abedon, Thomas-Abedon, Thomas, & Mazure, 2011) have raised serious doubts about Hankin's study being an early observation of effective phage-mediated antibacterial activity.

Frederick Twort should be credited for coming tantalizingly close to clearly discovering bacteriophages (Twort, 1915). His investigations led him to discover a small agent that infected and killed bacteria. However, apart from identifying it as a virus that grew on and subsequently killed the host bacteria, he also proposed the following two additional possible causes to explain his observations. These were: (a) a step in the life cycle of the bacteria or (b) an enzyme created by the bacteria themselves.

Alternate and indeed views orthogonal to d'Herelle were nurtured by many other scientists, most prominently by the Nobelists Jules Bordet and John Northrop, who hypothesized that these antibacterial or antimicrobial agents were inanimate chemicals or enzymes, that were already present in bacteria, and only initiated the activity of similar proteins, destroying the bacteria in the exercise. However, subsequent electron microscopy studies (Ruska, 1940) conclusively settled the debate in favor of d'Herelle. Unfortunately, d'Herelle died of cancer in 1949 and as a nearly forgotten man. He never won a Nobel Prize in spite of being nominated for it 28 times.

1.2 Lytic and Lysogenic Cycle

The life cycle or more precisely the reproduction cycle of a phage particle solely depends on its host bacterium. Broadly, the replication cycle of a bacteriophage could be of two types—lytic or lysogenic. Most of the phages are lytic phages. There are few phages called temperate phages that possess a unique ability to induce lysogenic cycle from the lytic cycle in some particular situations. The mechanism and the evolution of lysogenic cycle are much more complicated than that of the lytic cycle. The lytic cycle is a simple replication cycle comprised of five steps—attachment, penetration, replication, packaging, and burst out. The specificity of every step varies between different types of phages. Attachment of a phage particle on a host surface depends on some specific receptors on the host surface. Once a stable binding is achieved, a cascade of reactions initiates the process by which a phage particle inserts its genetic material inside the host cell. This procedure is followed by the replication and synthesis of various kinds of phage proteins depending on the type of genetic material of the phage (Weinbauer, 2004). Phage particles having a double-stranded or single-stranded DNA use the host machinery to reproduce their genetic material and other structural proteins. On the other hand, some of the RNA phages like retroviruses replicate their genetic material via DNA intermediate by using RNA-dependent DNA polymerase. Depending on the sense of their genome, other RNA phages replicate without forming DNA intermediate. Before replication of their genetic material and production of the structural proteins, phage particles extensively regulate host metabolic reactions. Subsequently, the formation of a new phage particle by the nascent structural proteins begins with the proper packaging of appropriate genetic material in it. This process varies from one phage to another and depends on the concatemeric sequence of the phage genome. This is followed by the release of new phage particles outside the host cell. On the other hand, in temperate phages, some particular conditions lead to lysogeny. In lysogeny, the genome of a phage particle gets integrated with the host chromosome at some special sites called attachment sites—after its insertion inside the host cell. After integration, the phage genome multiplies within the host genome with every cell division. This integrated version of phage genome within the host genome is called prophage. This lysogenic conversion occurs under certain conditions like low host cell density, low nutrient availability, etc. If the host cell density is low, the newly released phage particles will hardly find any uninfected host cell for a new infection. When suitable conditions—like an increase in the number of host cells or

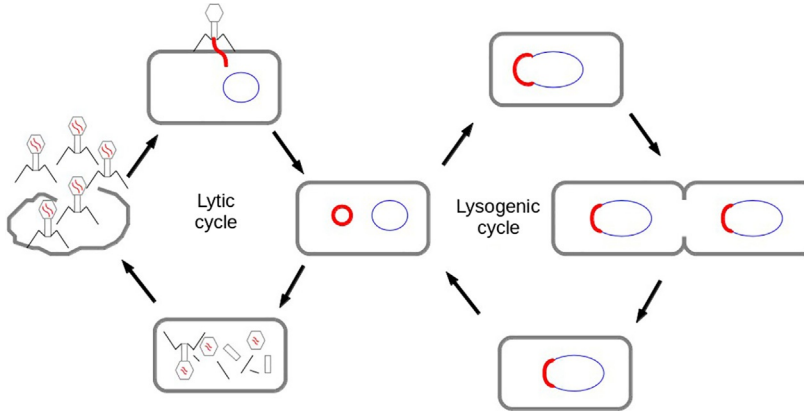

Fig. 1 Lytic and lysogenic cycle of phage.

removal of limitations on the amount of nutrients, arise again in future the prophages move their genome out of the host genome and replicate within the host cells for production of new phage particles. At this time it is very easy for newly formed phage particles to find an uninfected cell after release (Bertani, 2004). The lytic and lysogenic phage cycles are depicted in Fig. 1.

1.3 Adsorption Rate

There are various types of receptors present on the bacterial cell surface, where phage particles are adsorbed. The chemical nature of these receptors could vary from one species of bacteria to another as well as from one type of phage to another. The specificity of the bacteriophage and the host is primarily due to the uniqueness of the interaction of the phage with the host receptor. Modification of the host receptor is also responsible for phage-resistance property of the host cell (Etz, Minh, Schellack, Nagy, & Meinke, 2001; Labrie, Samson, & Moineau, 2010). Depending on the type of phage, the biochemical nature of the receptor molecule would also vary as can be observed from Fig. 2.

In phages T2 and T6 of *Escherichia coli*, receptors are mainly protein motifs—but in case of T3, T4, and T7, receptors with lipopolysaccharide components have been found (Randall-Hazelbauer & Schwartz, 1973). On the other hand, there are various types of receptors for *Salmonella* phages ranging from proteins like OmpC to flagella (Shin et al., 2012). The number of receptors on the surface of host cells or the receptor density varies from host to host and also depends on the growth medium of the host cell (Schwartz, 1976).

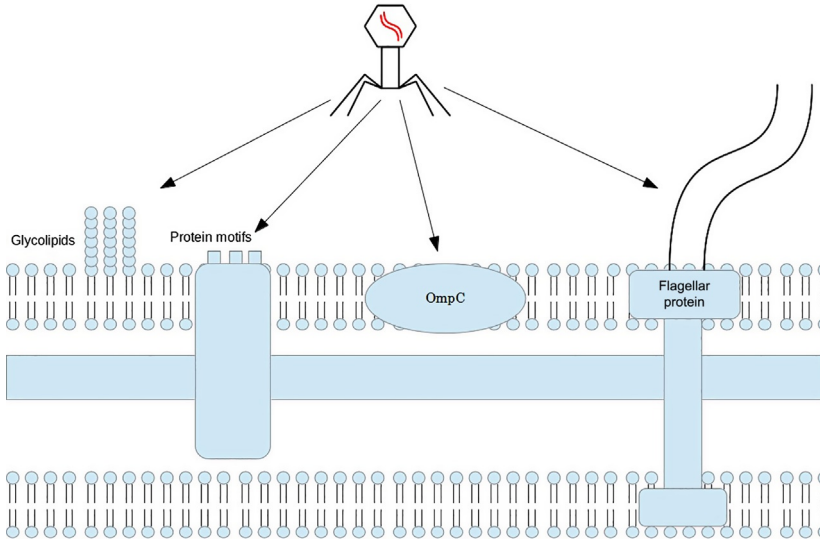

Fig. 2 Phage adsorption on various receptors.

A successful attachment of a particular bacteriophage with a particular receptor molecule on its host surface is a complex event guided by chance and depends on various types of parameters. It is dependent upon: (a) the affinity of the phage to irreversibly bind with the receptor, (b) the rate of diffusion of phage particles in the infection medium, and (c) the size of the host cells (Hyman & Abedon, 2009; Kropinski, 2009). An adsorption event can be quantitatively parameterized and can be expressed in terms of the adsorption rate constant. The adsorption rate is the probability of a phage particle to be irreversibly adsorbed on its host bacterium in unit volume of infection medium per unit time. This parameter is quantitatively expressed in units of mL per minute or mL per hour.

Mixing the appropriate amount of phages with its host bacteria in a suitable infection medium provides us a way for the experimental determination of phage adsorption rate. Mathematically, it is represented by the following equation:

$$N = \frac{-\ln\left(\frac{P}{P_0}\right)}{kt} \tag{1}$$

Here, P_0 and P are the phage densities at the beginning and at the end of the incubation of infection, respectively. N represents the initial host cell density and t the incubation time. The adsorption rate constant is

represented by k. Fig. 3 shows a typical plot of the number of free phages, plotted with time. The adsorption rate constant, k, is obtained from the plot in Fig. 3 as:

$$k = \frac{-\text{slope}}{N} \tag{2}$$

1.4 Multiplicity of Infection

The multiplicity of infection or MOI represents the ratio of the numbers of virus particles to the numbers of the host cells in a given infection medium. A value of MOI = 1 implies that on an average there is a single host cell for a single phage particle. However, in reality there can be multiple phage particles adsorbed on a single host cell, while some of the host cells might remain uninfected. The infection of a host cell by a phage particle is a chance event and can be statistically represented by the Poisson distribution (Ellis & Delbrück, 1939). Let us denote an arbitrary value of MOI by x. A bacterial population will be infected by phages such that the probability of a bacterium to be infected by y virus particles is denoted by:

$$P(y) = \frac{x^y e^{-x}}{y!} \tag{3}$$

So, for $x = 1$, $P(y)$ decreases as y increases. Therefore, the probability of a host bacterial cell to be infected by one phage particle at MOI equal to one is

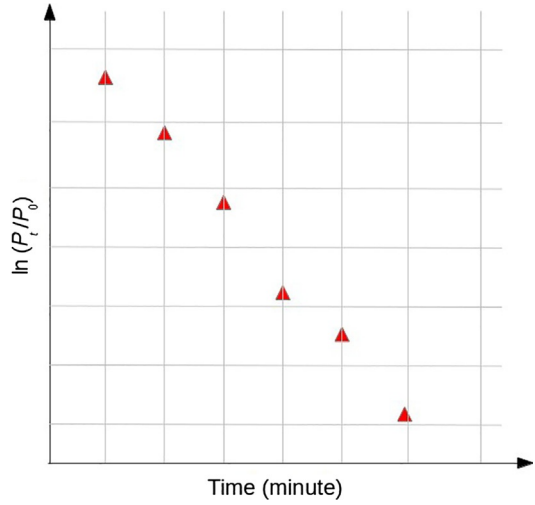

Fig. 3 Phage adsorption kinetics.

about 36.79%. Similarly, it can be calculated that the probability of a host bacterial cell to be infected by two or three phage particle at the same MOI is 18.39% and 6.13%, respectively.

1.5 One-Step Growth Curve

When a phage population in an infection medium infects a bacterial population, a chain of events is induced. New phage particles that are synthesized from an infected host cell can in turn infect other uninfected yet susceptible hosts. This sequence of events continues until a good number of these uninfected yet susceptible host cells are present in the infected medium. One round of the infection cycle is described as a characteristic one-step growth curve of bacteriophages, which is shown in Fig. 4.

Experimentally, the one-step growth curve can be obtained by diluting the mixture of phages and host bacterial cells—after adsorption of phages by the bacteria or by addition of substances that inhibit new infection (Ellis & Delbrück, 1939). It is obtained by plotting the numbers of free phages vs time. For a particular host and phage particle in a specific set of growth conditions and infection medium, the time taken for new phage particles to be released after successful adsorption is referred to as the latent period. There is another parameter called burst size, which is defined as the number of phage particles released from a host cell after a successful infection. In a one-step growth curve, we observe a sharp rise in free phage count, after the latent period. This increase of phage count is primarily due to the result of sequential bursting out of infected cells and release of the newly formed phage particles.

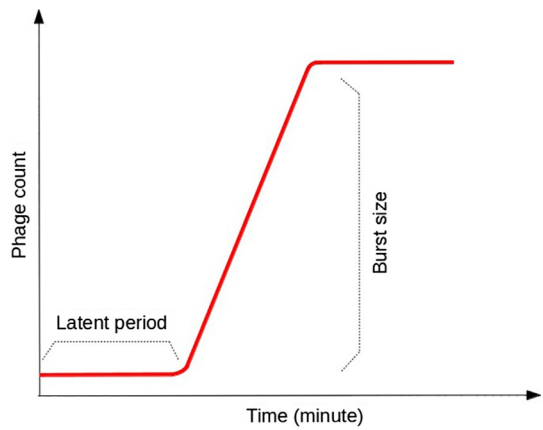

Fig. 4 One-step growth curve.

1.6 Phage Therapy

The emergence of antibiotic-resistant strains of life-threatening pathogenic microbes like *Mycobacteria* and *Salmonella* necessitates the use of other kinds of agents rather than employing the widespread practice of administration of antibiotics. In fact, the development of new antibiotics has also slowed down remarkably in the last few decades for a number of reasons. It is especially in the backdrop of these events that phage therapy presents a really promising alternative (Matsuzaki, Uchiyama, Takemura-Uchiyama, & Daibata, 2014; Reardon, 2014). Here, phage therapy implies the therapeutic use of phages as antibacterial agents. With the discovery of bacteriophages in 1917 along with the demonstration of their remedial potential, phage therapy was a subject of research over a period of about a decade and a half. However, the development of penicillin by Sir Alexander Fleming around 1928 severely impacted the ongoing research in this arena. Consequently, it remained out of vogue for a period of nearly 50 years—accelerated in no less measure by the outbreak of the Second World War. However, in certain areas of the erstwhile Union of Soviet Socialist Republics (USSR), notably in Georgia, various basic and applied (therapeutic) aspects of research on phages were practiced in quite some detail over the next few decades. Unfortunately, this body of research remained largely unrecognized and indeed somewhat unnoticed, perhaps also because the relevant yet countercurrent publications were not in English (Stone, 2002; Sulakvelidze, Alavidze, & Morris, 2001). At that time, most of the developed world was busy with developments in phage-based molecular biology techniques rather than the therapeutic aspects of phage administration. After that the importance of phage therapy was reemphasized by the work of Smith and Huggins (1982). The recent spotlight on the emergence of various antibiotic-resistant microbial strains and the huge health risks posed by them have led to some truly important developments in phage therapy, over the last decade.

A phase I safety trial of phage therapy for skin ulcers was approved and completed by the United States Food and Drug Administration in 2008 (Abedon, Kuhl, Blasdel, & Kutter, 2011). There have also been some successful trials for phage therapy for specific disease like cholera and infections with *Pseudomonas aeruginosa* and *Staphylococcus aureus* (Abedon, Kuhl, et al., 2011). Phage therapy has been shown to be effective against infection by *Mycobacterium ulcerans* in a murine footpad model (Trigo et al., 2013). Phage therapy is also known to be potentially effective in protecting honeybee larvae from American Foulbrood disease (Ghorbani-Nezami, LeBlanc, Yost, & Amy, 2015). Bacteriophage application has the potential to control water

contaminated with *Shigella* (Jun et al., 2016). In aquaculture, several examples of bacteriophage remediation of bacterial pathogens exist (Richards, 2014).

A schematic representation of various aspects of phage therapy is shown in Fig. 5.

Phage therapy offers various advantages over antibiotic treatment in many scenarios. First and foremost, the target specificity and precision of phage therapy is much higher than that of treatment with antibiotics. Antibiotics are not designed to kill merely the pathogenic bacteria at the target sites. At any prime antibiotic target site like the human gut there are various types of healthy flora also present. Apart from killing the pathogenic bacteria in the gut, antibiotics would also simultaneously target beneficial bacteria—which are rather crucial for maintaining healthy metabolism inside our intestine. However, bacteriophages being far more specific toward their target would in all likelihood destroy only the targeted pathogenic bacteria. The adopted route of administration is also a crucial factor during antibiotic use. So except tropical use, the antibiotics are delivered to the target sites mainly via the blood stream. So the amount of antibiotics consumed is usually larger than specifically required. They are also metabolized and leave the human body, so we need to take them at regular intervals. On the other hand, phages could multiply themselves at the target sites and are generally accompanied with minimal side effects (Cisek, Dąbrowska, Gregorczyk, & Wyzewski, 2017).

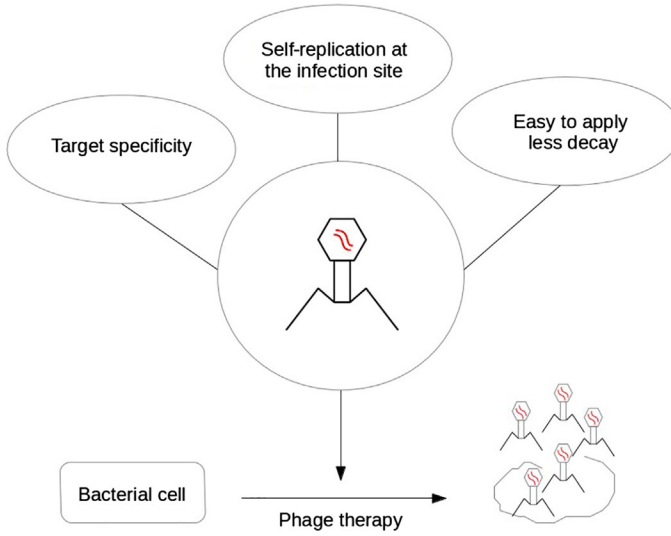

Fig. 5 Phage therapy.

1.7 Bacteria–Phage Coevolution

In the evolutionary run, the host bacterial cells try to evolve mechanisms that can resist phages. In their own defense phage particles also continually evolve new strategies for infecting the host bacteria, as a response. Extensive discussions on the general subject of bacteria–phage coevolution began at the turn of the last century in microbiology and were subsequently initiated in evolutionary biology, ecology, and other areas of theoretical biology. Bacteria–phage system is a good example of a system reflecting complex dynamics between the participants throughout the duration of interaction. One of the major problems in studying phages is to maintain their culture in the laboratory. Host cells also need to be cultured at the same time. As many of the bacteria are not amenable to being cultured in the laboratory, our knowledge of bacteria–phage competition and coevolution is somewhat limited. Such antagonistic coevolution is not so uncommon in nature. It can be observed in various places ranging from the human gut to the soil. It affects the microbial diversity in any type of environment to a great extent. Sometimes phages outnumber the population of their hosts, but most of the time they maintain a balance. Among various types of phage-resistant systems in bacteria, a newly discovered system is the CRISPR–CAS system (Barrangou et al., 2007). CRISPR stands for clustered regularly interspaced short palindromic repeats. Even this CRISPR system has also been antagonized by phage genes that can deactivate the CRISPR–CAS system (Bondy-Denomy, Pawluk, Maxwell, & Davidson, 2013).

1.8 Modeling Bacteria–Phage Interactions

As we discussed earlier, huge diversity is present in bacteria–phage interactions throughout nature. Naturally, it is not at all theoretically easy to comprehensively model such systems. Broadly, bacteria–phage interactions could be classified into two types depending upon the nature of the medium. In media with low viscosity like oceans, ponds, or rivers, which are rather abundant in nature or even in laboratory media like liquid broth—bacteria–phage interactions behave as a well-mixed population subject to minimal spatial limitations. On the other hand there are certain media, which possess high viscosity—examples of which are soil, tissue, solid agar media, and so on. In such scenarios, bacteria–phage interactions have spatial limitations and are not well mixed at any point of time during which they interact. Therefore, while modeling bacteria–phage interactions in media with low viscosity, the dependence of dynamics upon space is rather limited.

However, in highly viscous media, the resultant dynamics depends highly on the spatial constitution of the media.

In less viscous media, bacteria–phage interactions could be modeled as a set of ordinary differential equations (ODEs) or delay differential equations (DDEs). These differential equations would involve relations between the number/concentration of phages, infected bacteria, and uninfected yet susceptible bacteria and their derivatives with respect to time. Usually, parameters are also found in such relations involving two or more variables in these differential equations. In the present context parameters would be quantities like adsorption rate, growth rate, burst size, latent period, and so on. These systems can also be modeled using Monte Carlo simulations, which involve repeated, random, and exhaustive sampling from the space of all possible events.

On the other hand, in highly viscous media, bacteria–phage interactions are strongly dependent upon the spatial structure of the medium. Therefore, to model this system a series of reaction–diffusion equations could be employed where the phage and bacterial growth constitute the source terms, while phage diffusion in viscous media is captured by a diffusion term (Yin & McCaskill, 1992). It could also be modeled via cellular automata approach, where a grid of cells with changeable states evolves under some specific rules (Wei & Krone, 2005). A mathematical model of bacteria–phage interaction with immune response in the chemostat has also been recently formulated (Wang, 2017). Various aspects of modeling are shown in Fig. 6.

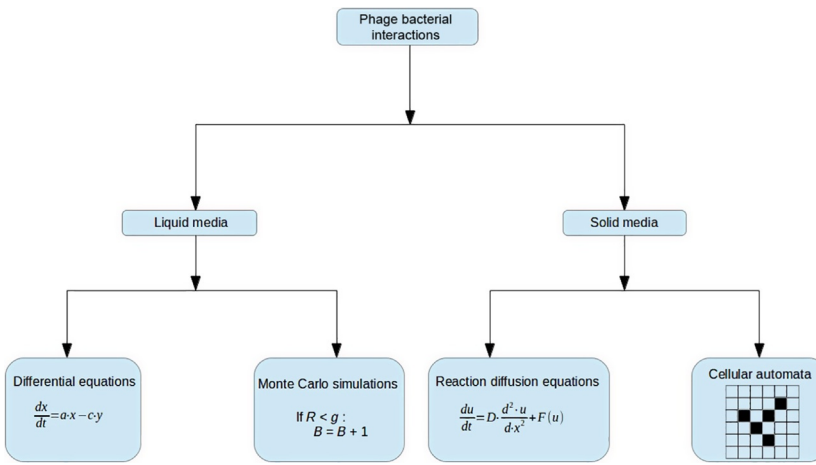

Fig. 6 Various aspects of modeling bacteria–phage interactions.

2. MATHEMATICAL MODELING

As aforementioned, the possibility of exploiting the infectious nature of the phages and using them as therapeutic agents against their host cells has generated renewed interest in host phage interactions. Therefore, various ingenious mathematical models provide us with an essential tool to understand the complex dynamics of bacteria–phage interactions. Computer simulations are also often employed in such studies of bacteria–phage interaction dynamics. Such modeling can shed significant insight and lead to interesting predictions, which could be useful in phage therapy. Almost all the models are based on the population dynamics of phages that are subject to the lytic cycle only and are usually deterministic in nature. A number of such models are based on the population dynamics of prey–predator models and epidemiological infection models. It is very helpful and instructive to obtain the basic parameters used in mathematical modeling from the experimental data obtained under controlled conditions in the laboratory. The extraction of parameters from experimental data may provide valuable clues toward understanding the characteristic kinetics of bacteria–phage interactions, in much more complex setups.

2.1 Differential Equations

A differential equation is used to mathematically define the relation between a given function and its derivatives. Differential equations involving derivatives of quantities with respect to time are often used to describe dynamical systems, especially when the interest lies in studying the evolution of such systems with time. While modeling dynamical systems, the derivative usually represents the rate of change of a variable of the system under consideration. In general, real-world systems are usually quite complex in nature and it is naturally impossible to model them taking all their details into account. Construction of equations governing the dynamical behavior of a given system requires framing proper mathematical equations involving the relevant variables and parameters. For example, in bacteria–phage dynamics—the number of infected host cells, free phage particles, and uninfected yet susceptible bacterial cells are considered as variables. Parameters are part of the relations involving two or more variables in an equation. In the present context, parameters would be quantities like growth rate, burst size, adsorption rate, latent period, and so on.

Inclusion of too many variables or values to be calculated, while constructing the equations to describe a system—might render the equations very hard to solve analytically. Therefore, the main idea behind modeling a system is to construct a minimum set of equations using variables and parameters that describe the physical system completely or at least to a fair approximation. At the same time it should be enough to capture the essence of the dynamics of the system. If the data obtained by the set of equations are in "good" agreement with the experimentally measured data, then predictions drawn from the model could successfully point toward the behavior of the system at longer timescales. In case the modeled equations result in predictions, which are far from actually observed behavior—the equations should be modified and rewritten with increased rational and practical reasoning. It is very important to note here that approximations and simplifications could greatly help in getting analytically tractable solutions for many if not most models. However, such analytically obtained solutions should obviously be checked against real experimental data. Differential equations can be classified into various types such as ordinary differential equations (ODEs), partial differential equations (PDEs), and delay differential equations (DDEs). While ODEs contain derivatives which depend upon the value of a function at the present time, DDEs are a type of differential equations in which the derivative of a function at any given point of time, t, is dependent upon the value of the function at a time prior to t and not merely upon the current time, t. A DDE can be written as:

$$x'(t) = f(t, x(t), x(t-\tau_1), x(t-\tau_2), \ldots, x(t-\tau_k)), \tag{4}$$

where time delays τ_1, τ_2, and τ_k are positive constants. Also, for ODEs, the value of the function at initial point, say $t = t_0$, is sufficient to determine its solution, whereas DDEs require the "history" of the system, i.e., solution at time points prior to the initial time points, τ_1, τ_2, …, τ_k along with the solution at the initial point t_0 (Shampine & Thompson, 2001). Thus, DDEs are sometimes considered to be more realistic than ODEs where the dynamics of a system is only based upon the current state of the variables.

In population dynamics, the time involved in biological processes such as gestation, maturity, or time to be able to reproduce plays a very crucial role. Such scenarios are quite common in real-world systems. For example, in a prey–predator model, the birth rate of predators may depend upon both current and the previous number of predators and preys. Thus, a DDE provides a rather effective way to model and successfully gain significant insights on the dynamics of a system.

DDEs can be solved numerically, and the most popular approach is to use explicit Runge–Kutta methods. A number of DDE solving programs and packages are also available presently. A few of the commonly used ones are dde23 in MATLAB® (Shampine, 1994), DDE solver for FORTRAN 90 and FORTRAN 95 (Thompson & Shampine, 2006) and pydelay in python (Flunkert & Schoell, 2009).

2.2 Basic Model for Bacteria–Phage Interactions

The paper by Campbell (1961) was among the first to introduce mathematical modeling using DDEs toward understanding the kinetics of bacteria–phage interactions. Campbell modeled the bacteria–phage population dynamics under chemostat-like conditions as interacting populations of susceptible uninfected bacteria, S, and free phage, P, which he related as:

$$\dot{S}(t) = \alpha S(t)\left[1 - \frac{S(t)}{C}\right] - kS(t)P(t) - aS(t) \tag{5}$$

$$\dot{P}(t) = bkS(t-\tau)P(t-\tau) - \mu_p P(t) - aP(t) \tag{6}$$

Here, susceptible bacterial cells grow at a constant rate α with the carrying capacity of bacterial population being C. It should be noted that the infection of bacterial cells occurs by irreversible adsorption of free phage particles in susceptible bacterial cells at rate "k" and is treated according to the principle of mass action. This principle alludes to the fact that in a well-mixed population the rate of contact of two groups is proportional to the product of population size of both the groups concerned. Susceptible bacteria as well as free phages are removed from the system at a constant flow rate, a. Thus, Eq. (5) gives the change in susceptible bacterial concentration. The phage kinetics is somewhat more complicated as infected cells are lysed after a fixed latent period τ, i.e., at a time, τ, after infection—resulting in an average release of b new phage particles per infected cell, with b being referred to as the burst size. μ_p denotes the rate of spontaneous inactivation of phage particles, and the overall equation for phage concentration is given by Eq. (6). The effect of growth rate of phages on the population of phages and bacteria was observed using this model. It was shown that a slow growth rate of phages leads to dying out of the phage particles, whereas a rapid growth rate of phages maintains bacteria at a low nonzero level along with the phages. Further, the effect of phage survival in competing host environment was also studied. In this case, the bacterial population does not die out as phages continue to survive by simply choosing the "best-adapted" out of

the population of competing hosts. The above model was further extended by modeling bacteria–phage dynamics as three interacting populations—susceptible uninfected bacteria, S, infected bacteria, I, and free phages, P (Levin, Stewart, & Chao, 1977). They also considered a model with two preys and one predator and studied the stable states of coexistence for each of the two preys and also the sole predator in the heterogeneous population.

2.3 Resource Concentration Factor

Lenski and Levin (1985) incorporated an additional state r for resource concentration in their host phage model in a chemostat to study the dynamics of bacteria–phage interactions built with a view to gain insight into evolutionary constraints for coexistence of *E. coli* bacteria and virulent phage. Their model is described as follows:

$$\dot{r}(t) = D(r_0 - r(t)) - \alpha(r)\varepsilon S(t) \tag{7}$$

$$\dot{S}(t) = \alpha(r)S(t) - kS(t)P(t) - DS(t) \tag{8}$$

$$\dot{I}(t) = kS(t)P(t) - e^{-D\tau}kS(t-\tau)P(t-\tau) - DI(t) \tag{9}$$

$$\dot{P}(t) = be^{-D\tau}kS(t-\tau)P(t-\tau) - kS(t)P(t) - DP(t) \tag{10}$$

Here, $\alpha(r)$ denotes the growth rate of uninfected bacteria, while ε is the amount of resources consumption by a new bacterium. The bacterial population as well as the phage population is washed out of the system at a constant rate D. The fraction of bacteria that was infected τ time ago but has not yet been washed out of the system and is denoted by $e^{-D\tau}$. The interpretation of the remaining parameters is the same as the previously described model. This model is based over the following assumptions, namely: (1) infected cells cannot be infected again and (2) infected cells can neither grow nor use resources.

2.4 Phage Resistance in Bacteria

It has been observed that phage adsorption depends upon the number of receptors on the bacterial cell wall (Berg & Purcell, 1977; Moldovan, Chapman-McQuiston, & Wu, 2007). To incorporate these findings, Chapman-McQuiston and Wu (2008) introduced heterogeneity in bacterial population depending upon their response to phage infection while studying the population dynamics of *E. coli* bacterium and λ-phage. Bacteria with the same number of receptors possess same sensitivity to phage infection. Thus, bacterial population was divided into subpopulations B_n, where $0 < n < N_{\max}$

depends upon the number of phage receptors, n. Each subpopulation consists of sensitive cells, S_n, and infected cells, I_n, with adsorption coefficient γ_n. The model is given as:

$$\dot{S}_n(t) = \alpha S_n - \gamma_n P S_n + \sum_{m=0}^{N_{\max}}{}' \alpha_{mn} S_m - \left(\sum_{m=0}^{N_{\max}}{}' \alpha_{mn} \right) S_n \tag{11}$$

$$\dot{I}_n(t) = \gamma_{n+1}(S_{n+1} + I_{n+1})P - \gamma_n I_n P - \varepsilon I_n \tag{12}$$

$$\dot{P}(t) = mP(t-\tau)\sum_{n=0}^{N_{\max}} \gamma_n S_n(t-\tau) - P\sum_{n=0}^{N_{\max}} \gamma_n (S_n + I_n) \tag{13}$$

Partitioning of receptor cells due to cell division leads to switching between the subpopulations and is represented by α_{mn}, which denotes the switching rate from subpopulation n to subpopulation m. The prime symbol in the summations denotes exclusion of the case when $m = n$. The growth rate for all bacterial subpopulations is assumed to be identical. Incorporation of population heterogeneity improves fitness of the bacterial populations against phage infection and thereby makes it possible for the bacterial population to persist under strong phage pressure.

Cairns, Timms, Jansen, Connerton, and Payne (2009) introduced bacterial mutation rate denoted by f, thus assimilating phage-resistant bacteria, R into the model system given by:

$$\dot{S}(t) = \alpha S(t) - fS(t) - kS(t)P(t) \tag{14}$$

$$\dot{R}(t) = \alpha R(t) + fS(t) \tag{15}$$

$$\dot{I}(t) = kS(t)P(t) - kS(t-\tau)P(t-\tau) \tag{16}$$

$$\dot{P}(t) = bkS(t-\tau)P(t-\tau) - kS(t)P(t) - \mu_p P(t) \tag{17}$$

Unlike, the models mentioned earlier—here, the growth factor, α, accounts for both replication and phage-independent bacterial cell death. The following assumptions have been made in the concerned model system: (1) resistant bacteria are totally resistant to phages and once resistance is acquired—it cannot be lost and (2) sufficient concentration of resources is available so as to avoid competition between susceptible and resistant bacteria. Here, it was shown that for the decline in susceptible bacteria population, the free phage population must exceed a minimum threshold called the inundation threshold. On the other hand, only when the susceptible bacterial population exceeds a given threshold, namely, proliferation threshold—the phage population rises in number.

Han and Smith (2012) modeled the dynamics of phage-sensitive (S) and phage-resistant (M) bacteria to understand persistence and extinction of bacterial strains and phages in a chemostat. The cost of resistance to phage infection was included in form of low nutrient uptake by the phage-resistant bacteria compared to the phage-sensitive bacteria thereby resulting in reduced growth rate of the phage-resistant bacteria. The system was modeled by following sets of equations:

$$\dot{r}(t) = D(r_0 - r(t)) - \gamma_s f_s(r(t))S(t) - \gamma_M f_M(r(t))M(t) \tag{18}$$

$$\dot{S}(t) = f_s(r(t))S(t) - kS(t)P(t) - DS(t) \tag{19}$$

$$\dot{M}(t) = f_M(r(t))M(t) - DM(t) \tag{20}$$

$$\dot{I}(t) = kS(t)P(t) - DI(t) - k\int_0^\infty e^{-D\tau}S(t-\tau)P(t-\tau)d\nu(\tau) \tag{21}$$

$$\dot{P}(t) = -kS(t)P(t) - DP(t) + k\int_0^\infty e^{-D\tau}b(\tau)S(t-\tau)P(t-\tau)d\nu(\tau) \tag{22}$$

Here, $f_s(r)$ and $f_M(r)$ denotes nutrient uptake functions for S and M, respectively, with $f_s(r) > f_M(r)$. D is the dilution rate, γ_s and γ_M are constants, and ν is a probability measure.

2.5 Bacteria–Phage Interaction Networks

Instead of following the well-traveled route of studying phage bacteria interactions as coupled interactions in isolation, recent work has attempted to introduce systems approaches to study these interactions at a network level (Flores, Meyer, Valverde, Farr, & Weitz, 2011; Weitz et al., 2013). Network approaches have been successfully applied to a plethora of problems in biology ranging from neuronal networks to protein–protein interactions (Banerjee & Roy, 2012; Banerjee, Sinha, & Roy, 2015). Also, at the level of individual proteins, residue interaction graphs or protein contact networks have been used with success to model such proteins as networks (Grewal, Mitra, & Roy, 2015; Grewal & Roy, 2015). They have also been used with success in biomedical imaging and noninvasive diagnostics (Banerjee, Azharuddin, et al., 2015).

It has been shown that available host phage infection networks demonstrate a characteristic nested structure and are statistically different from random networks (Flores et al., 2011). Antibiotic treatment has been observed to expand the resistance reservoir and ecological network of the phage metagenome, and broad bacterial functions are enriched in phage

metagenomes following drug perturbation in mice (Modi, Lee, Spina, & Collins, 2013). That, coevolutionary diversification creates nested-modular structure in phage bacteria interaction networks has also been demonstrated (Beckett & Williams, 2013).

As bacteriophages are the most abundant biological entities in our gut, they should be given due consideration in our pursuit of personalized medicine. There exists a plethora of interactions in the human gut: interactions between host, bacteria, and phages (Khan Mirzaei & Maurice, 2017). Network level studies on human gut phageome (HGP) have revealed that it plays a critical role in maintaining the proper function of a stable, balanced gut microbiome. HGP is significantly decreased in individuals with gastrointestinal disease like ulcerative colitis and Crohn's disease (Manrique et al., 2016).

2.6 System of ODEs

To understand the density-dependent qualities of bacteria–phage interactions, Payne and Jansen (2001) studied a system of ODEs with time-dependent variables $H(t)$ and $h(t)$. $H(t)$ and $h(t)$ represents the host responses against the bacteria and against the phages, respectively, thereby capturing the role of host in generic manner. The following is the set of ODEs proposed to model phage therapy:

$$\dot{S} = \alpha S - kSP - H(t)S \tag{23}$$

$$\dot{I} = \alpha I + kSP - \mu_i I - H(t)I \tag{24}$$

$$\dot{P} = b\mu_i I - kSP - \mu_p P - h(t)P \tag{25}$$

Here, the replication rates for uninfected as well as infected bacteria are assumed to be identical. μ_i is the degradation rate of infected bacteria or lysis rate. Several important threshold values including phage proliferation threshold value, clearance threshold were calculated with each resulting in different therapy outcomes. In passive therapy, which depends on the concentration of phages—lysis due to primary infection caused by inoculated phages is a prime reason for removal of a major part of the bacterial population. On the other hand, in active therapy, which depends upon the concentration of bacteria—elimination of bacteria is caused mainly by secondary infection due to phages released by lysis.

Another model was proposed to study the dynamics of interaction in which the ability of phage to lyse host cells decreases as they approach their carrying capacity (Weitz & Dushoff, 2008).

$$\dot{S}(t) = \alpha S(t)\left[1 - \frac{S(t)}{C}\right] - kS(t)P(t)\left[1 - \frac{mS(t)}{C}\right] - dS(t) \tag{26}$$

$$\dot{P}(t) = bkS(t)P(t)\left[1 - \frac{mS(t)}{C}\right] - \mu_p P(t) \tag{27}$$

Here, α denotes the fractional reduction in cell lysis, and the density-independent death rate is given by d. The model results in alternative stable states where initial population conditions determine either the coexistence or the overall phage extinction.

Multiple phage adsorptions in host cell were analyzed by considering a nontrivial model involving ODEs (Smith & Trevino, 2009). This system allows for adsorption of multiple phages upon a single bacterial host cell. In this model, for both phage and bacteria to persist, the identified basic reproduction number must exceed unity. Also, the number of phages adsorbing to a bacterial cell follows the binomial distribution. The mean of the distribution increases slowly with time.

2.7 Recent Developments

In a recent study, modeling the dynamics of *Salmonella* phage and its pathogenic host, variation in latent period and adsorption rate were introduced instead of considering them as constant as was the case with previous models (Santos, Carvalho, Azeredo, & Ferreira, 2014). The incorporation of latent period in form of a normal distribution and adsorption rate as a function of the bacterial growth rate results in better agreement between the data obtained by numerical solutions and experimental observations. This makes it possible to accurately predict the behavior of bacteria–phage dynamics.

In a recent paper (Samaddar et al., 2016), a new mechanism, namely, that of secondary killing for cell death in addition to the primary mechanism of cell lysis, has been proposed. The phage host system modeled was mycobacteriophage D29 and *Mycobacterium smegmatis*. Further experimental results in the system verified that phage infection leads to production of superoxide radicals, which are released upon the lysis of host cells. Reactive oxygen species (ROS) thus generated contribute toward the host bacterial cell death as a secondary factor. This process of phage-mediated secondary killing is depicted in Fig. 7.

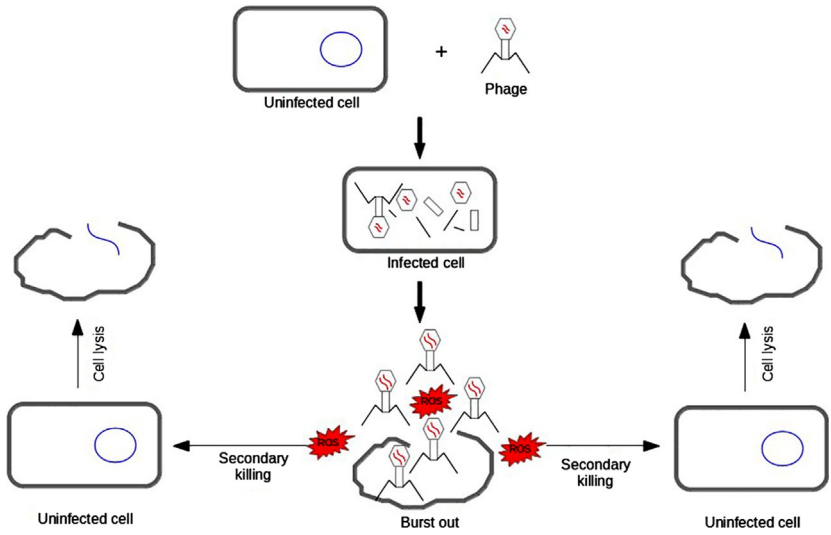

Fig. 7 Phage-mediated secondary killing of bacteria.

It was also shown that only a fraction of the infected cells gets lysed, and the MOI plays an important role in both the cases. The proposed model can be represented by the following set of DDEs:

$$\frac{dS}{dt} = \underbrace{\alpha S(t)}_{\text{cell growth}} - \underbrace{kS(t)P(t)}_{\substack{\text{cell decay due} \\ \text{to adsorption}}} - \underbrace{qmkS(t-\tau)P(t-\tau)S(t)\exp\left[{}^{-t}/_{(a\tau)}\right]\text{Heavi}(t-\tau)}_{\text{secondary cell decay due to release of superoxide from lysed bacteria}} \tag{28}$$

$$\frac{dI}{dt} = \underbrace{kS(t)P(t)}_{\substack{\text{infected cells} \\ \text{due to adsorption}}} - \underbrace{mkS(t-\tau)P(t-\tau)\text{Heavi}(t-\tau)}_{\substack{\text{fraction of cells lysed} \\ \text{(infected cell population decay due to lysis)}}} \tag{29}$$

$$\frac{dP}{dt} = \underbrace{b}_{\text{burst size}} \underbrace{mkS(t-\tau)P(t-\tau)\text{Heavi}(t-\tau)}_{\substack{\text{fraction of cells lysed resulting} \\ \text{in new phages}}} - \underbrace{kS(t)P(t)}_{\substack{\text{phage decay due to adsorption}}} \tag{30}$$

Here, m is the fraction of the infected cells lysed. The parameter q was introduced in the system of DDEs to capture the effect of the "secondary killing factor" released in the environment. This is responsible for *secondary cell death* arising from the procedure proposed herein apart from the

well-known primary mechanism of host cell lysis. The effect of this secondary killing and its dependence upon the susceptible cell population as a function of time is given by:

$$D_{\text{secondary}} \propto S(t) e^{\frac{-t}{a\tau}} \tag{31}$$

where a is a constant.

3. COMPUTER SIMULATIONS

Computer simulations, sometimes also referred to as numerical simulations, represent a process, which attempts to mimic the actual behavior of a system. Usually this is accompanied by a clever application of various types of algorithms. Sometimes, a computer simulation is interchangeably used with the terms "numerics" or "numerical solutions" in biological literature. A numerical solution can be thought of as a process of approximately solving different mathematical equations obtained after the mathematical modeling of a system—often on a computer. Needless to mention, closed form or exact analytical solutions would have been rather difficult to obtain in most of such scenarios.

There are various types of computer simulations among which Monte Carlo is one of the most extensively studied methods. Other than that there are various other kinds of simulations like agent-based simulations, continuous dynamic simulations, discrete event simulations, etc.

3.1 Monte Carlo Simulations

Monte Carlo simulation is a class of numerical simulations where repeated sampling of a huge sample space on a random basis is employed to obtain results. It is named after the Monte Carlo casino located in Monaco, France. It is widely used across the sciences from physics to biology and in engineering, marketing, finance, and transport to name a few areas (Kroese, Brereton, Taimre, & Botev, 2014). It is especially helpful in the area of decision making and risk analysis where the chance of occurrence of an event is very important. As aforementioned, repeated random sampling is the core idea by which we implement probabilistic principles to solve a wide range of deterministic problems. Stanislaw Ulam invented the version of Monte Carlo simulations as we use them today. It must also be mentioned that the famous Italian physicist and Nobel Prize winner Enrico Fermi also experimented with the ideas

associated with Monte Carlo simulations, even though he did not really publish in this area. Stanislaw Ulam and John Von Neumann used these methods on an ENIAC computer during the development of the atom bomb project at Los Alamos National Laboratory. In the Markov chain Monte Carlo (MCMC) method, which is named after the Russian mathematician Andrey Markov, random samples are drawn from a known stationary probability distribution. Here, the probability distribution is constructed by taking into account the probability of occurrence of each event in a finite number of steps (Hastings, 1970). This MCMC could predict the possibility of an immediately subsequent event depending merely on the present event and the given probability distribution. This means it would not retain or use the memory of previous events. MCMC method has diverse applications in the field of computational biology and computational physics.

Here, we present a very simple example of Monte Carlo simulations—namely to estimate the value of "π," which is the ratio of the circumference to the diameter of any circle. To estimate the value of "π" we will consider a circle inside a square as shown in Fig. 8.

The circle can be divided into four quadrants and the square into four equal parts. We denote the smaller square by Sq_{small}. Every side of Sq_{small} equals R, which is also the radius of the given circle. For simplicity, let us focus on only one quadrant. Let us conceive of a machine, which can imprint and count the tiniest of dots in a given area. We let this device

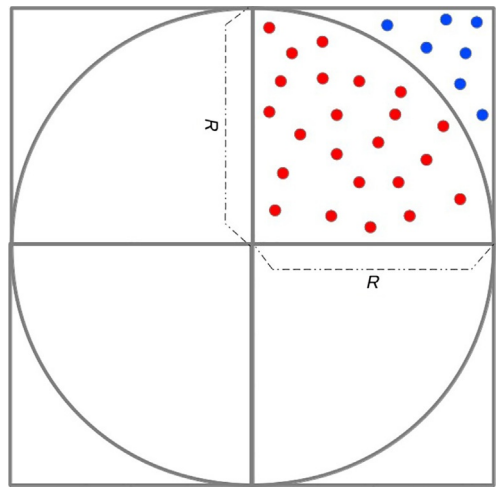

Fig. 8 A simple example of Monte Carlo simulations.

imprint a good number ($\sim 10^5$ or more) of dots purely at random inside the smaller square, $\mathrm{Sq}_{\mathrm{small}}$, which is presently under our consideration. We then let our machine count the total number of dots inside the quadrant and the total number of dots inside the smaller square. Obviously, the latter will include dots located not just in the quadrant contained in the smaller square but also dots located outside it. For the moment, let us neglect all dots lying right on the boundaries of the quadrant or the square—which even if accounted will not alter our findings in any remarkable manner. As aforementioned, "π" is four times the ratio of the area of the quadrant to the area of the smaller square. Equivalently, in the present scenario, we would find that to a very good approximation it would be four times the ratio of the number of dots inside the smaller square to the number of dots in the quadrant, as counted by our device.

Now, how do we simulate this process on a computer? For our simulations, let us use a random number generator, which uniformly generates two random numbers between 0 and R, at every step of the simulation. These two numbers would represent the abscissa, x, and ordinate, y, of each dot imprinted by our machine. The distance of the position of each dot from the center of the circle is then calculated as $d = +\sqrt{(x^2 + y^2)}$. If this distance, d, is less than or equal to the radius, R, of our circle—then the dot obviously lies inside the quadrant of our circle or on its boundary. Let us call this event A. When the distance, d, is greater than the radius, R, of our circle, it is obviously located outside the quadrant but still within or at most on the boundary of the smaller square. We denote this event as B. We separately keep track of the number of times each of these events, A and B occur and denote these as N_A and N_B, respectively. Let us repeat this process for 10^5 or more times on the computer and calculate $4N_A/(N_A + N_B)$. We would again find that this ratio is tantalizingly close to π, the determination of which has been the singular aim of our elaborate exercise.

3.2 Probability Distribution

Probability or the chance of the occurrence of an event is one of the central ideas of Monte Carlo simulations. Here, we take a cursory glance at how the properties of a system can be described by a probability distribution function, which is often simply referred to as the probability distribution. The probability of occurrence of various outcomes of a given system under different conditions is represented by the probability distribution. It is usually expressed as a function of a particular independent random variable or in

some cases by more than one random variable, which may or may not be correlated among each other.

In statistics, probability distributions can be either discrete or continuous depending upon the nature of the sample space. In a discrete probability distribution, possible outcomes are always captured by a discrete set of numbers or events. Examples of discrete probability distributions can be observed in case a coin is repeatedly flipped or a dice is rolled many times. A probability mass function is a function that gives the probability that a *discrete* random variable is exactly equal to a given value. However, in continuous probability distributions the value of a possible outcome could be any real number, albeit within a certain interval.

The most straightforward type of probability distribution is the uniform probability distribution, where each event in the distribution has the same probability of occurrence. There are of course many other known examples of probability distributions. Binomial distribution, Poisson distribution, and Normal or Gaussian distribution are among the most important and frequently used probability distributions, especially the last one.

The binomial distribution is a type of discrete probability distribution, which has only two independent and mutually exclusive outcomes—say "*success*" and "*failure*"—each with a given probability. Here, probability mass function is used and has two parameters n and p. The number of independent trials is denoted by n, whereas p is the probability of one of the two outcomes. The probability of the other outcome can be denoted by q, where q is obviously equal to $(1-p)$ since there are only two outcomes. If the number of one of the two given outcomes viz "success" is x, in a total number of n trials, then the probability mass function is represented as:

$$P(x) = {}^{n}C_{x} \cdot p^{x} \cdot q^{(n-x)} \tag{32}$$

The Poisson distribution is also a type of discrete probability distribution, which represents the chance of occurrence of rather rare events. It is mainly used in scenarios where the number of total events is very large but the probability of success is rather small. In this probability distribution, the mean, m, and the variance of the sample space is known to be identical. Here, Eq. (3), which has been mentioned earlier, represents the probability of a rare and random variable x:

$$P(x) = \frac{e^{-m} \cdot m^{x}}{x!} \tag{3}$$

On the other hand, normal distribution is a continuous probability distribution. Here, the highest frequencies are concentrated around the center

of the distribution. Frequency decreases as the ends of the distribution are approached. It is widely used to model many real-world phenomena associated with randomness. It is also referred to as Gaussian distribution after the German mathematician Carl Gauss who is supposed to have discovered it. The graphical representation of the normal distribution looks like a bell-shaped curve, which is symmetrical at both ends. This symmetry gives rise to an exactly identical value of the three central tendencies of any given distribution—namely mean, median, and mode. With the central tendency of μ, whose value is democratically shared by the mean, median, and mode of the distribution along with a standard deviation of σ, the probability density function of the normal distribution is represented as:

$$P(x) = \frac{1}{\sqrt{2 \cdot \pi \cdot \sigma^2}} \cdot e^{\frac{-(x-\mu)^2}{2 \cdot \sigma^2}} \tag{33}$$

3.3 Probability of Cell Division

Bacteria replicate by binary fission. In this process, after replication of the genetic material in an exact copy, a bacterial cell gets split into two cells, with each cell possessing a copy of the replicated genetic elements. A bacterial population is made up of many bacterial cells, which could vary in their age, metabolic state, etc. So when we are considering the growth in population at a particular time step, we also have to take into account the event of every cell division at that specific time step. When we are considering a large bacterial population, it is quite apparent that all the cells do not simultaneously undergo cell division at the very same instant of time (Dwek, Kobrin, Grossman, & Ron, 1980).

Experimentally, we can determine the specific growth rate, μ, of bacteria, where the specific growth rate is measured in the log phase. In the log phase, the bacterial population growth is subject to first-order reaction kinetics and depends on the number of existing bacterial cells at a particular time instant. Bacterial cell count can be directly measured by a count of colony-forming units or indirectly by optical density measurements. Now within a specific time Δt in the log phase, if the change in the number of cells is ΔN, then the specific growth rate, μ, can be calculated as follows:

$$\mu = \frac{\Delta(\ln N)}{\Delta t} \tag{34}$$

The specific growth rate has a unit of t^{-1}. It also represents the probability of cell division. For example, let us suppose that a bacterial culture has the specific growth rate 0.3 per minute. It implies that a particular cell inside the population has a probability of 0.3 for binary fission in every minute. Now, to simulate the system using Monte Carlo methods, we would use this number as the probability for cell division. In our simulations—at every time step we will generate a random number, R_w, from a uniform distribution between 0 and 1. Depending on the system under study, it could also be drawn from any other predefined distributions. If R_w is less than the probability of binary fission, i.e., the specific growth rate, the cell divides.

3.4 Probability of Phage Adsorption

We have discussed the complexity of phage adsorption on a host cell surface earlier in Sections 1.3 and 1.4 of this chapter. This process is affected by various factors ranging from the affinity of phage particles for receptor molecules to the rates of diffusion in the medium of infection. Here, the MOI also plays a vital role as it denotes the number of phages per host cell. An MOI of 1 indicates that on an average for every host cell there is an adsorbed phage particle. However, in a real infection medium a host cell may get infected by more than one phage particle. In fact it may not even be infected by a phage particle at all. The probability of a host cell to be affected by a phage particle can be well represented by the Poisson distribution (Ellis & Delbrück, 1939). At an MOI equal to x, the probability that a host cell getting infected by y phage particles is captured by:

$$P(y) = \frac{x^y e^{-x}}{y!} \tag{3}$$

For an MOI equal to 1, the probability that a phage particle infects a host cell is 0.36. But for a lower MOI like 0.05, the probability of a host cell getting infected by a phage particle is about 0.048. Therefore, for our Monte Carlo simulations, we can use this number as the probability of adsorption or probability of infection. To simulate such infection events, at every time step—for every host cell we generate a random number, R_a from a uniform distribution. Now if the value of R_a is less than the adsorption rate—the host cell is understood as infected by a phage. If a host cell has not yet been infected by a phage particle, we would check whether the cell could divide (Levin, Moineau, Bushman, & Barrangou, 2013; Samaddar et al., 2016), as discussed earlier in Section 3.3.

3.5 Latent Period and Burst Size

The latent period is the time taken by a phage particle to reproduce inside an infected host cell. At the population level in a one-step growth curve, it can be represented as the time taken for the newly formed phage particles to appear in the media. The number of newly synthesized phage particles from an infected cell is called the burst size. From the moment of infection to the bursting out of an infected host cell—a phage particle will try to reproduce its genome and also to synthesize the relevant structural proteins, so as to form new phages. Both latent period and burst size depend on the host cell, infecting phage, and the incubation conditions. As described earlier in Section 1.5, from one-step growth experiments, we can directly measure the latent period and the burst size. However, for the burst size measurement, we have to divide the count of plaque-forming units (PFU) at saturation of the one-step growth curve by the number of host cells at the beginning of the experiment. For example, if we start with 5×10^5 host cells and at the saturation of the one-step growth curve the PFU count is1.5×10^8, the burst size will be approximately 300.

3.6 Secondary Infection and Killing

Infected cells burst out to release new phage particles, which carry the potential of reinfection. However, all infected cells would not burst out simultaneously at a single time step. A percentage of cells that get infected—burst out after the latent period. This percentage is decided by the host species, incubation conditions, and MOI. In case of *M. smegmatis* MC2155 and mycobacteriophage D29, the infection in low MOI results in about 10% of the infected cells to burst out after the latent period (Samaddar et al., 2016). There are also few reported mechanisms in the same system, where infected cells produce certain ROS. Due to this release, some of the uninfected host cells in the vicinity also get killed as collateral damage. This is depicted in Fig. 7.

We attempt to incorporate this entire process in our Monte Carlo simulations in the following manner. At each time step 10% of the infected cells burst out after the latent period. An infected cell will produce new phage particles exactly identical to the burst size. The effects of ROS which kills a portion of neighboring cells are quantified by the ratio of the number of uninfected cells to the number of infected cells.

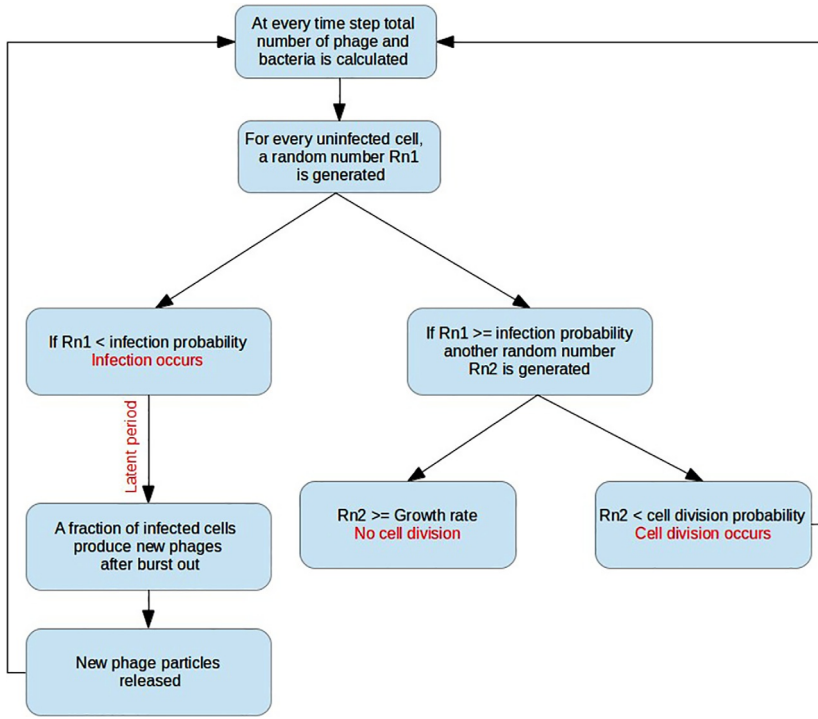

Fig. 9 Algorithm for Monte Carlo simulation of bacteria–phage dynamics.

Fig. 9 represents the overall algorithm of the Monte Carlo simulation of bacteria–phage interaction.

In conclusion—the obvious purpose of computer simulations is to gain a better understanding of any given system. In experiments, we can usually observe the behavior of a system. However, there are various limitations due to which we cannot predict or often even understand the internal mechanisms at work in the system, beyond a certain extent. But when we simulate a system, it confers the ability to gain some "understanding" and even predict the behavior of a system—in response to changes in various parameters. Sometimes, this can lead to better experimental design, at least in accessible experimental regions dictated by parameters of the model. The problem detailed here (Samaddar et al., 2016) presents a good example of how simulations and modeling help in designing experiments, which can shed valuable insight into the overall behavior of the system. The experimentally verified findings of the secondary killing mechanism were made possible only due to modeling and simulation efforts.

4. PHAGE BACTERIA INTERACTION UNDER SPATIAL LIMITATIONS

Earlier in this chapter, we discussed about bacteria–phage interactions in liquid media or broth and various aspects of modeling such interactions. Interactions in a liquid medium or broth represent a well-mixed population dynamics, which can be adequately dealt without the inclusion of subtleties of the underlying spatial structure. However, in many other environments like soil ecosystems, animal or plant tissues, and bacterial biofilms, there are various kinds of spatial restraints influencing bacteria–phage interactions. A higher viscosity of the medium would impose spatial constraints, as a result of which the phage population would not adequately mix with the bacterial population and the interactions remain spatially constrained.

4.1 Formation of Plaque

The spatially influenced interactions between bacteria and phages can be studied in the formation of plaques by bacteriophages on the bacterial lawn. Such plaque formations are not only studied to understand the spatial interactions in bacteria–phage systems—they are also widely used as a technique to count the phage number in phage population dynamics (Ellis & Delbrück, 1939). Experimentally plaques can be obtained by pour plate technique method on soft agar. In this method, diluted phage solution is mixed with pure host population, termed as indicator bacteria. The bacteria–phage mixture is then mixed with 0.4%–0.8% agar media, called soft agar or top agar. Subsequently, the mixture is poured on the standard 1.5%–2% thin hard agar plate and incubated at the proper temperature, overnight. After incubation, the host population on soft agar is likely to produce a bacterial lawn atop the agar substrate. However, some small clear zones are likely to appear and these are referred to as plaques. The dynamics behind the plaque formation is as follows. The phages infect the bacterial cells and produce new phage particles after bursting out from infected host cells. These newly formed phage particles are now ready to infect the neighboring susceptible bacteria resulting in a "clear zone" at the point of infection inside the cloudy host lawn as represented in Fig. 10. The number of plaques indicates the number of phages in the diluted phage solution and is called plaque-forming unit or PFU.

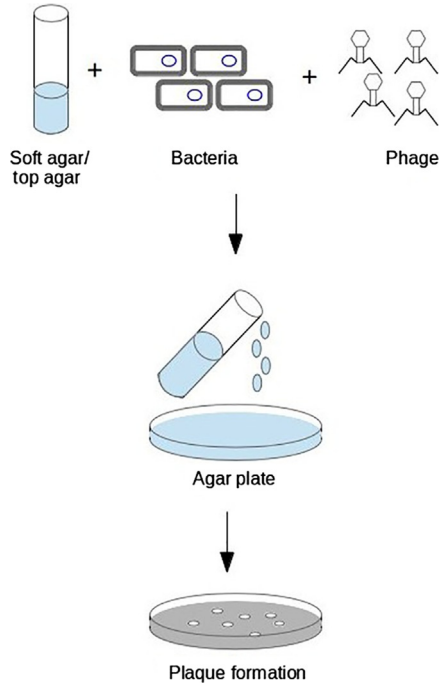

Fig. 10 Plaque formation on agar.

4.2 Factors Affecting Plaque Diameter

Plaque formation inside soft agar is a complex phenomenon dictated by various factors. We will discuss these factors one by one in the sequential order of their role in plaque formation. Inside the soft agar, the adsorption events of phage particles on host surfaces depend on the adsorption rate constant, host density, agar density, and latent period (Abedon & Yin, 2009). The greater the host density, the faster does adsorption of phage particles occur. This also indicates that the probability of the adsorption of phage particles increases with the host density. Also, higher agar density decreases the media porosity, which in turn retards phage diffusion through agar. After the first round of infection, the newly released phage particles gain the ability to infect neighboring host bacteria. The burst size should also be counted as a function of plaque growth after the initial rounds of infection. The higher the burst size, greater is the density of phages near a host cell—thereby increasing the probability of adsorption in the later round of infections. On the other hand, lower density of indicator bacteria negatively affects the plaque growth. The insufficient formation of bacterial lawn due to the initial low cell density makes it difficult to identify

the "clear" plaque formation zones on the agar plate. It has been observed that phages with short and long latent periods would produce smaller plaques compared to phages with medium latent period (Gallet, Kannoly, & Wang, 2011). Though phages with higher adsorption rates can easily counter the host in the initial stages, overall, an increase in the adsorption rate at later time has a negative effect on the plaque diameter. Phages possessing higher adsorption rates diffuse in a slower manner thereby resulting in a smaller plaque diameter (Abedon & Yin, 2009; Gallet et al., 2011).

4.3 Modeling of Plaque Growth as a Reaction–Diffusion System

As discussed earlier, various factors are responsible for plaque formation. To model the dynamics of plaque formation, various approaches have been undertaken. Initially, adsorption rate and the burst size were ignored while modeling plaque formation. The phage diffusion rate, D, and the latent period, L, were the only parameters considered to affect the size of the plaque. The rate of plaque enlargement, R, was described (Kaplan, Naumovski, Rothschild, & Collier, 1981) as:

$$R = x \cdot \left(\frac{D}{L}\right)^{\frac{1}{2}} \tag{35}$$

Here, x represents the binding constant of phages.

A more mechanistic approach involves reaction–diffusion equations to model the interaction between the free phages, V, the host cells, B, and the infected hosts, I. Burst size, Y, is also considered along with various rate constants like k_1, k_2, and k_3, which, respectively, represent adsorption constant, bacteria–phage dissociation constant, and the death rate of infected bacteria. The overall reaction equation is:

$$V + B \underset{k_2}{\overset{k_1}{\leftrightarrow}} I \xrightarrow{k_3} Y \cdot V \tag{36}$$

Depending on the above equation, the system of equations for the concentrations of V, B, and I as a function of $\vec{r}$ and t is given by:

$$\frac{\delta[V]}{\delta t} = D \cdot \frac{\delta^2[V]}{\delta r^2} + \frac{D}{r}\left(\frac{\delta[V]}{\delta r}\right) - k_1[V][B] + k_2[I] + Yk_3[I] \tag{37}$$

$$\frac{\delta[B]}{\delta t} = -k_1[V][B] + k_2[I] \tag{38}$$

$$\frac{\delta[I]}{\delta t} = k_1[V][B] - k_2[I] - k_3[I] \tag{39}$$

4.4 Traveling Wave Front Solutions

This system of three coupled equations from Eqs. (37) to (39) represents a reaction–diffusion system of bacteria–phage interactions on an agar plate as a function of time and space. A traveling wave front solution for this system can be obtained with a coordinate $\vec{z} = \vec{r} - \vec{C} \cdot \vec{t}$, where the front velocity is represented by C. At equilibrium, where the adsorption and phage dissociation processes are much faster than the death rate of the infected host, the front velocity is given by:

$$C_{\text{eq}} = 2 \cdot \left[\frac{D \cdot k_3 \cdot (Y-1) \cdot f \cdot K_m}{(1 + f \cdot k_m)^2} \right]^{\frac{1}{2}} \tag{40}$$

Here, N_0 and N_m represent the initial lawn density and the highest lawn density reached by the bacteria. The other terms are $f = N_0/N_m$ and $K_m = (k_1 \cdot N_m)/k_2$. The above expression is also used to study hindered diffusion of phages (Yin & McCaskill, 1992).

4.5 Cellular Automata Modeling

Cellular automata is a class of discrete and individual agent-based modeling systems, applied in a variety of fields ranging from engineering and physics to theoretical biology. In this type of modeling, a finite number of cells are generally considered on a one-dimensional or two-dimensional lattice, though three-dimensional cellular automata is also used (Chopard & Droz, 1998). In the lattice, there is a fixed number of possible states available for each cell. This type of modeling is very useful when the state of a cell is considered as a function of time as well as space. John Von Neumann and Stanislaw Ulam are first thought to have proposed it in 1940 at the Los Alamos National Laboratory. Decades later, mathematician John Horton Conway devised a famous cellular automaton called the Game of Life, also popularly known simply as Life. Subsequently Stephen Wolfram argued about the huge potential of cellular automata techniques.

Depending on the dimensionality of the lattice considered, every cell has a definite number of neighbors. In one dimension, the radial neighborhood is the most commonly used method for defining the neighborhood of a cell. It specifies the number of cells on either side of the central cell. There are various well-known neighborhood methods in two dimensions like Von Neumann neighborhood method or Moore neighborhood method. Von Neumann neighborhood method is the smallest and simplest

neighborhood method in two dimensions. It consists of the cell itself and the cells at a Manhattan distance of 1. Considering the coordinate of the central cell as (0,0), its neighborhood, according to the Von Neumann neighborhood method, can be described as:

$$N = [(0, -1), (-1, 0), (0, 0), (+1, 0), (0, +1)] \tag{41}$$

On the other hand, in the Moore neighborhood method the coordinates of the neighbors would be given by:

$$N = [(-1, -1), (0, -1), (1, -1), (-1, 0), (0, 0), (+1, 0), (-1, +1), (0, +1), (1, +1)] \tag{42}$$

Initially, each cell is assigned a particular state. At every time step, each cell changes its state depending on the state of its neighbor by some fixed set of rules. The system is then evolved over a period of time. Other than the methods mentioned earlier, there are few other neighborhood methods like Margolus neighborhood method, Hexagonal neighborhood method, etc. The basic neighborhood methods discussed earlier are shown in Fig. 11.

4.6 SIR-Type Modeling

Spatially restricted bacteria–phage interactions can be modeled upon SIR class of models, which are widely used in epidemiology. SIR might refer to "susceptible, infected, recovered" or "susceptible, infected, removed." They are also used in modeling of interacting particle systems or IPS (Wei & Krone, 2005; White, Del Rey, & Sánchez, 2007). In SIR, on a two-dimensional grid, a finite number of cells is considered. Each cell can have three possible states, susceptible, *S*, infected, *I*, and removed or

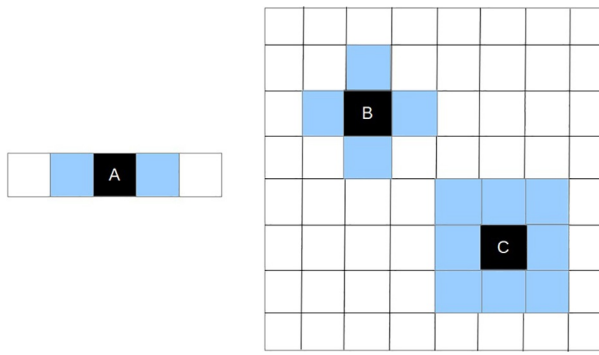

Fig. 11 (A) Radial neighborhood, (B) Von Neumann neighborhood, and (C) Moore neighborhood in cellular automata.

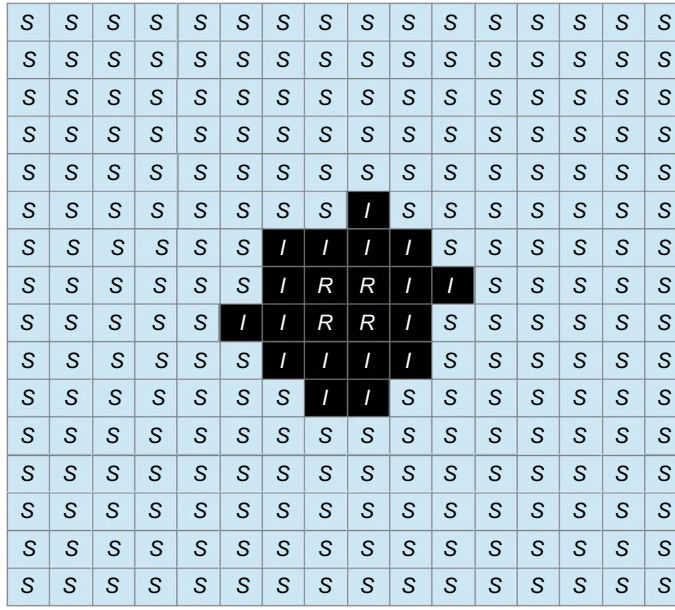

Fig. 12 Simulating plaque growth by cellular automata.

recovered, *R*. Initially, all cells are susceptible in nature, *S*, with the exception of a single infected cell occupying a random position on the grid. At each subsequent time step, neighboring susceptible cells become infected depending on a predefined mathematical function which is defined by the phage adsorption rate, latent period, burst size, and phage diffusion as described in Fig. 12. Most of the rates can be experimentally determined in the laboratory. This kind of modeling is occasionally also referred to as probabilistic cellular automata in literature.

When a phage particle infects a saturated population of susceptible hosts at a particular point, a wave of infection is generated from the point of infection. This type of wave propagation can be modeled by reaction-diffusion equations. The main purpose of this variety of modeling is to quantify the rate of spreading of infection and its ultimate fate. The effects of various types of mutant invasions inside a population can also be studied using such models (Wei & Krone, 2005).

ACKNOWLEDGMENTS

Senior Research Fellowships provided to R.K.G. and S.S. by the University Grants Commission of India supported this work. We thank Prof. Devrani Mitra of Presidency University, Kolkata for her critical reading of our manuscript.

REFERENCES

Abedon, S. T., Kuhl, S. J., Blasdel, B. G., & Kutter, E. M. (2011). Phage treatment of human infections. *Bacteriophage*, *1*(2), 66–85.

Abedon, S. T., Thomas-Abedon, C., Thomas, A., & Mazure, H. (2011). Bacteriophage prehistory: Is or is not Hankin, 1896, a phage reference? *Bacteriophage*, *1*(3), 174–178.

Abedon, S. T., & Yin, J. (2009). Bacteriophage plaques: Theory and analysis. In *Isolation, characterization, and interactions: Vol. 1. Bacteriophages: Methods and protocols* (pp. 161–174). http://www.springer.com/gp/book/9781588296825.

Banerjee, S. J., Azharuddin, M., Sen, D., Savale, S., Datta, H., Dasgupta, A. K., et al. (2015). Using complex networks towards information retrieval and diagnostics in multidimensional imaging. *Scientific Reports*, *5*, 17271.

Banerjee, S. J., & Roy, S. (2012). Key to network controllability. *arXiv*. 1209.3737. https://arxiv.org/pdf/1209.3737.

Banerjee, S. J., Sinha, S., & Roy, S. (2015). Slow poisoning and destruction of networks: Edge proximity and its implications for biological and infrastructure networks. *Physical Review E*, *91*(2), 022807.

Barrangou, R., Fremaux, C., Deveau, H., Richards, M., Boyaval, P., Moineau, S., et al. (2007). CRISPR provides acquired resistance against viruses in prokaryotes. *Science*, *315*(5819), 1709–1712.

Beckett, S. J., & Williams, H. T. P. (2013). Coevolutionary diversification creates nested-modular structure in phage–bacteria interaction networks. *Interface Focus*, *3*, 20130033.

Berg, H. C., & Purcell, E. M. (1977). Physics of chemoreception. *Biophysical Journal*, *20*(2), 193–219.

Bertani, G. (2004). Lysogeny at mid-twentieth century: P1, P2, and other experimental systems. *Journal of Bacteriology*, *186*(3), 595–600.

Bondy-Denomy, J., Pawluk, A., Maxwell, K. L., & Davidson, A. R. (2013). Bacteriophage genes that inactivate the CRISPR/Cas bacterial immune system. *Nature*, *493*(7432), 429–432.

Cairns, B. J., Timms, A. R., Jansen, V. A. A., Connerton, I. F., & Payne, R. J. H. (2009). Quantitative models of in vitro bacteriophage-host dynamics and their application to phage therapy. *PLoS Pathogens*, *5*(1), e1000253.

Campbell, A. (1961). Conditions for the existence of bacteriophage. *Evolution*, *15*(2), 153–165.

Chapman-McQuiston, E., & Wu, X. L. (2008). Stochastic receptor expression allows sensitive bacteria to evade phage attack. Part II: Theoretical analyses. *Biophysical Journal*, *94*(11), 4537–4548.

Chopard, B., & Droz, M. (1998). *Cellular automata*. Springer.

Cisek, A. A., Dąbrowska, I., Gregorczyk, K. P., & Wyzewski, Z. (2017). Phage therapy in bacterial infections treatment: One hundred years after the discovery of bacteriophages. *Current Microbiology*, *74*(2), 277–283.

d'Herelle, F. (1917). Sur un microbe invisible antagoniste des bacilles dysentériques. *Comptes Rendus. Académie des Sciences*, *165*, 373–375.

Duckworth, D. H. (1976). Who discovered bacteriophage? *Bacteriological Reviews*, *40*(4), 793–802.

Dwek, R. D., Kobrin, L. H., Grossman, N., & Ron, E. Z. (1980). Synchronization of cell division in microorganisms by percoll gradients. *Journal of Bacteriology*, *144*(1), 17–21.

Ellis, E. L., & Delbrück, M. (1939). The growth of bacteriophage. *The Journal of General Physiology*, *22*(3), 365–384.

Etz, H., Minh, D. B., Schellack, C., Nagy, E., & Meinke, A. (2001). Bacterial phage receptors, versatile tools for display of polypeptides on the cell surface. *Journal of Bacteriology*, *183*(23), 6924–6935.

Flores, C. O., Meyer, J. R., Valverde, S., Farr, L., & Weitz, J. S. (2011). Statistical structure of host–phage interactions. *Proceedings of the National Academy of Sciences of the United States of America*, *108*(28), E288–297.

Flunkert, V., & Schoell, E. (2009). Pydelay—A python tool for solving delay differential equations. *arXiv* preprint arXiv:09111633. https://arxiv.org/pdf/0911.1633.pdf.

Gallet, R., Kannoly, S., & Wang, N. (2011). Effects of bacteriophage traits on plaque formation. *BMC Microbiology*, *11*(1), 181.

Ghorbani-Nezami, S., LeBlanc, L., Yost, D. G., & Amy, P. S. (2015). Phage therapy is effective in protecting honeybee larvae from American Foulbrood disease. *Journal of Insect Science*, *15*(1), 84.

Grewal, R. K., Mitra, D., & Roy, S. (2015). Mapping networks of light-dark transition in LOV photoreceptors. *Bioinformatics*, *31*(22), 3608–3616.

Grewal, R. K., & Roy, S. (2015). Modeling proteins as residue interaction networks. *Protein and Peptide Letters*, *22*(10), 923–933.

Han, Z., & Smith, H. L. (2012). Bacteriophage-resistant and bacteriophage-sensitive bacteria in a chemostat. *Mathematical Biosciences and Engineering*, *9*(4), 737–765.

Hankin, E. H. (1896). L'action bactericide des eaux de la Jumna et du Gange sur le vibrion du cholera. *Annales de l'Institut Pasteur*, *10*(5), 511–523.

Hastings, W. K. (1970). Monte Carlo sampling methods using Markov chains and their applications. *Biometrika*, *57*(1), 97–109.

Hyman, P., & Abedon, S. T. (2009). Practical methods for determining phage growth parameters. In *Isolation, characterization, and interactions: Vol. 1. Bacteriophages: Methods and protocols* (pp. 175–202). Humana Press. http://www.springer.com/in/book/9781588296825.

Jun, J. W., Giri, S. S., Kim, H. J., Yun, S. K., Chi, C., Chai, J. Y., et al. (2016). Bacteriophage application to control the contaminated water with Shigella. *Scientific Reports*, *6*, 22636.

Kaplan, D. A., Naumovski, L., Rothschild, B., & Collier, R. J. (1981). A model of plaque formation. *Gene*, *13*(3), 221–225.

Khan Mirzaei, M., & Maurice, C. F. (2017). Ménage à trois in the human gut: Interactions between host, bacteria and phages. *Nature Reviews Microbiology*, *15*, 397–408.

Kroese, D. P., Brereton, T., Taimre, T., & Botev, Z. I. (2014). Why the Monte Carlo method is so important today. *Wiley Interdisciplinary Reviews: Computational Statistics*, *6*(6), 386–392.

Kropinski, A. M. (2009). Measurement of the rate of attachment of bacteriophage to cells. In *Isolation, characterization, and interactions: Vol. 1. Bacteriophages: Methods and protocols* (pp. 151–155). Humana Press. http://www.springer.com/in/book/9781588296825.

Labrie, S. J., Samson, J. E., & Moineau, S. (2010). Bacteriophage resistance mechanisms. *Nature Reviews Microbiology*, *8*(5), 317–327. https://doi.org/10.1038/nrmicro2315.

Lenski, R. E., & Levin, B. R. (1985). Constraints on the coevolution of bacteria and virulent phage: A model, some experiments, and predictions for natural communities. *American Naturalist*, *125*(4), 585–602.

Levin, B. R., Moineau, S., Bushman, M., & Barrangou, R. (2013). The population and evolutionary dynamics of phage and bacteria with CRISPR-mediated immunity. *PLoS Genetics*, *9*(3), e1003312.

Levin, B. R., Stewart, F. M., & Chao, L. (1977). Resource-limited growth, competition, and predation: A model and experimental studies with bacteria and bacteriophage. *The American Naturalist*, *111*(977), 3–24.

Manrique, P., Bolduc, B., Walk, S. T., van der Oost, J., de Vos, W. M., & Young, M. J. (2016). Healthy human gut phageome. *Proceedings of the National Academy of Sciences of the United States of America*, *113*(37), 10400–10405.

Matsuzaki, S., Uchiyama, J., Takemura-Uchiyama, I., & Daibata, M. (2014). Perspective: The age of the phage. *Nature*, *509*(7948), S9.
Mc Grath, S., & van Sinderen, D. (Eds.), (2007). *Bacteriophage: Genetics and molecular biology*: Horizon Scientific Press/Caister Academic Press.
Modi, S. R., Lee, H. H., Spina, C. S., & Collins, J. J. (2013). Antibiotic treatment expands the resistance reservoir and ecological network of the phage metagenome. *Nature*, *499*, 219–222.
Moldovan, R., Chapman-McQuiston, E., & Wu, X. L. (2007). On kinetics of phage adsorption. *Biophysical Journal*, *93*(1), 303–315.
Payne, R. J. H., & Jansen, V. A. A. (2001). Understanding bacteriophage therapy as a density-dependent kinetic process. *Journal of Theoretical Biology*, *208*(1), 37–48.
Randall-Hazelbauer, L., & Schwartz, M. (1973). Isolation of the bacteriophage lambda receptor from *Escherichia coli*. *Journal of Bacteriology*, *116*(3), 1436–1446.
Reardon, S. (2014). Phage therapy gets revitalized: The rise of antibiotic resistance rekindles interest in a century-old virus treatment. *Nature*, *510*(7503), 15–17.
Richards, G. P. (2014). Bacteriophage remediation of bacterial pathogens in aquaculture: A review of the technology. *Bacteriophage*, *4*(4), e975540.
Ruska, H. (1940). Die Sichtbarmachung der bakteriophagen lyse im übermikroskop. *Naturwissenschaften*, *28*(3), 45–46.
Samaddar, S., Grewal, R. K., Sinha, S., Ghosh, S., Roy, S., & Das Gupta, S. K. (2016). Dynamics of mycobacteriophage-mycobacterial host interaction: Evidence for secondary mechanisms for host lethality. *Applied and Environmental Microbiology*, *82*(1), 124–133.
Santos, S. B., Carvalho, C., Azeredo, J., & Ferreira, E. C. (2014). Population dynamics of a Salmonella lytic phage and its host: Implications of the host bacterial growth rate in modelling. *PLoS One*, *9*(7), e102507.
Schwartz, M. (1976). The adsorption of coliphage lambda to its host: Effect of variations in the surface density of receptor and in phage-receptor affinity. *Journal of Molecular Biology*, *103*(3), 521–536.
Shampine, L. F. (1994). Numerical solution of ordinary differential equations (Vol. 4). CRC Press.
Shampine, L. F., & Thompson, S. (2001). Solving delay differential equations with DDE23. *Applied Numerical Mathematics*, *37*(4), 441–458.
Shin, H., Lee, J. H., Kim, H., Choi, Y., Heu, S., & Ryu, S. (2012). Receptor diversity and host interaction of bacteriophages infecting Salmonella enterica serovar Typhimurium. *PLoS One*, *7*(8), e43392.
Smith, H. W., & Huggins, M. B. (1982). Successful treatment of experimental Escherichia coli infections in mice using phage: Its general superiority over antibiotics. *Microbiology*, *128*(2), 307–318.
Smith, H. L., & Trevino, R. T. (2009). Bacteriophage infection dynamics: Multiple host binding sites. *Mathematical Modelling of Natural Phenomena*, *4*(6), 111–136.
Stone, R. (2002). Stalin's forgotten cure. *Science*, *298*(5994), 728–731.
Sulakvelidze, A., Alavidze, Z., & Morris, J. G. (2001). Bacteriophage therapy. *Antimicrobial Agents and Chemotherapy*, *45*(3), 649–659.
Summers, W. C. (2012). The strange history of phage therapy. *Bacteriophage*, *2*(2), 130–133.
Thompson, S., & Shampine, L. F. (2006). A friendly Fortran DDE solver. *Applied Numerical Mathematics*, *56*(3–4), 503–516.
Trigo, G., Martins, T. G., Fraga, A. G., Longatto-Filho, A., Castro, A. G., Azeredo, J., et al. (2013). Phage therapy is effective against infection by *Mycobacterium ulcerans* in a murine footpad model. *PLoS Neglected Tropical Diseases*, *7*(4), e2183.
Twain, M. (1897). *More tramps abroad* (pp. 343–345). London: Chatto & Windus.
Twort, F. W. (1915). An investigation on the nature of ultra-microscopic viruses. *The Lancet*, *186*(4814), 1241–1243.

Wang, W. (2017). Dynamics of bacteria-phage interactions with immune response in a chemostat. *Journal of Biological Systems*, *25*, 697.
Wei, W., & Krone, S. M. (2005). Spatial invasion by a mutant pathogen. *Journal of Theoretical Biology*, *236*(3), 335–348.
Weinbauer, M. G. (2004). Ecology of prokaryotic viruses. *FEMS Microbiology Reviews*, *28*(2), 127–181.
Weitz, J. S., & Dushoff, J. (2008). Alternative stable states in host-phage dynamics. *Theoretical Ecology*, *1*(1), 13–19.
Weitz, J. S., et al. (2013). Phage–bacteria infection networks. *Trends in Microbiology*, *21*(2), 82–91.
White, S. H., Del Rey, A. M., & Sánchez, G. R. (2007). Modeling epidemics using cellular automata. *Applied Mathematics and Computation*, *186*(1), 193–202.
Yin, J., & McCaskill, J. S. (1992). Replication of viruses in a growing plaque: A reaction-diffusion model. *Biophysical Journal*, *61*(6), 1540–1549.